Mycoscience 61 (2020) 184–189

Contents lists available at ScienceDirect

Mycoscience

journal homepage: www.elsevier.com/locate/myc

Full paper

Morphological and molecular identification of two new species of *Tubulicrinis* (Hymenochaetaceae, Hymenochaetales) from southern China

Xiao He [a, c], Zheng-Jun Shi [a], Chang-Lin Zhao [a, b, c, d, *]

[a] Key Laboratory of State Forestry Administration for Highly-Efficient Utilization of Forestry Biomass Resources in Southwest China, Southwest Forestry University, Kunming, 650224, PR China
[b] Key Laboratory for Forest Resources Conservation and Utilization in the Southwest Mountains of China, Ministry of Education, Southwest Forestry University, Kunming, 650224, PR China
[c] College of Biodiversity Conservation, Southwest Forestry University, Kunming, 650224, PR China
[d] Key Laboratory of Forest Disaster Warning and Control of Yunnan Province, Southwest Forestry University, Kunming, 650224, PR China

ARTICLE INFO

Article history:
Received 6 January 2020
Received in revised form
27 March 2020
Accepted 30 March 2020
Available online 3 April 2020

Keywords:
Molecular phylogeny
Taxonomy
Wood-inhabiting fungi
Yunnan Province

ABSTRACT

Two new wood-inhabiting fungal species, *Tubulicrinis xantha* and *T. yunnanensis* spp. nov., are described based on morphological and molecular characters. *Tubulicrinis xantha* is characterized by resupinate, furfuraceous basidiomata with buff to yellowish hymenial surface, amyloid lyocystidia and cylindrical to allantoid, hyaline, thin-walled, smooth basidiospores (5.3–6.3 × 1.2–1.6 μm). *Tubulicrinis yunnanensis* is characterized by pruinose basidiomata with primrose to olivaceous hymenial surface and encrusted lyocystidia and cylindrical, hyaline, thin-walled, smooth basidiospores (4.2–6.2 × 1.2–2 μm). Sequences of ITS and LSU nrRNA gene regions of the studied samples were generated, and phylogenetic analyses were performed with maximum likelihood, maximum parsimony and bayesian inference methods. The phylogenetic analyses based on molecular data of ITS and ITS + nLSU sequences showed that *T. xantha* grouped with *T. martinicensis*, and *T. yunnanensis* grouped with *T. glebulosus*.

1. Introduction

Tubulicrinis Donk (Hymenochaetaceae, Hymenochaetales) is typified by *T. glebulosus* (Fr.) Donk (Donk, 1956), and is characterized by resupinate basidiomata, firmly adnate, smooth, pruinose to porulose hymenophore, a monomitic hyphal system with clamped connections on generative hyphae and conspicuous, projecting, amyloid cystidia and small basidia, and cylindrical to allantoid or globose to ellipsoid, thin-walled, smooth, IKI− (both inamyloid and indextrinoid), acyanophilous basidiospores (Bernicchia & Gorjón, 2010; Donk, 1956). So far about 46 species have been accepted in the genus worldwide (Crous et al., 2016; Cunningham, 1963; Donk, 1956; Eriksson, 1958; Gruhn, Hallenberg, & Courtecuisse, 2016; Hayashi, 1974; Hjortstam, 1981, 2001; Hjortstam, Larsson, Ryvarden, & Eriksson, 1988; Oberwinkler, 1966; Rajchenberg, 2002; Ryvarden, 1975; Sharma, Singh, & Dhingra, 2015).

Molecular studies involving *Tubulicrinis* have been carried out (Crous et al., 2016; Dai, 2011; Larsson et al., 2006). The research on molecular phylogeny for the hymenochaetoid clade revealed that two *Tubulicrinis* species: *T. gracillimus* (Ellis & Everh. ex D.P. Rogers & H.S. Jacks.) G. Cunn. and *T. subulatus* (Bourdot & Galzin) Donk, formed a monophyletic lineage and then grouped with *Coltricia* clade and Hymenochaetaceae clade (Larsson et al., 2006). A revised checklist of corticioid and hydnoid fungi in China showed that six *Tubulicrinis* species were recorded in this area (Dai, 2011). Six new *Tubulicrinis* species were nested into the Tubulicrinaceae clade belonging to the order Hymenochaetales (Crous et al., 2016).

During investigations on wood-inhabiting fungi in southern China, two additional taxa were found which could not be assigned to any described species. In this study, the authors expand samplings from previous studies to examine taxonomy and phylogeny of this new species within the *Tubulicrinis*, based on the internal transcribed spacer (ITS) regions and the large subunit nuclear ribosomal RNA gene (nLSU) sequences.

* Corresponding author. Key Laboratory of State Forestry Administration for Highly-Efficient Utilization of Forestry Biomass Resources in Southwest China, Southwest Forestry University, Kunming 650224, PR China.
E-mail address: fungichanglinz@163.com (C.-L. Zhao).

https://doi.org/10.1016/j.myc.2020.03.008
1340-3540/

2. Materials and methods

2.1. Morphological studies

The specimens studied are deposited at the herbarium of Southwest Forestry University, Kunming, Yunnan Province, P.R. China (SWFC). Macromorphology descriptions are based on field notes. Colour terms follow Petersen (1996). Micromorphology was studied on the dried specimens, and observed under a light microscope (Dai, 2012). The following abbreviations were used: KOH = potassium hydroxide 5% water solution, CB = Cotton Blue, CB− = acyanophilous, IKI = Melzer's reagent, IKI− = both inamyloid and indextrinoid, L = mean spore length (arithmetic average of all spores), W = mean spore width (arithmetic average of all spores), Q = variation in the L/W ratios between the specimens studied, n (a/b) = number of spores (a) measured from given number (b) of specimens.

2.2. Molecular procedures and phylogenetic analyses

The EZNA HP Fungal DNA Kit (Omega Biotechnologies Co., Ltd, Kunming, Yunnan Province) was used to obtain PCR products from dried specimens, according to the manufacturer's instructions with some modifications. ITS region was amplified with primer pair ITS5 and ITS4 (White, Bruns, Lee, & Taylor, 1990). Nuclear LSU region was amplified with primer pair LR0R and LR7 (http://www.biology.duke.edu/fungi/mycolab/primers.htm). The PCR procedure for ITS was as follows: initial denaturation at 95 °C for 3 min, followed by 35 cycles at 94 °C for 40 s, 58 °C for 45 s and 72 °C for 1 min, and a final extension of 72 °C for 10 min. The PCR procedure for nLSU was as follows: initial denaturation at 94 °C for 1 min, followed by 35 cycles at 94 °C for 30 s, 48 °C 1 min and 72 °C for 1.5 min, and a final extension of 72 °C for 10 min. The PCR products were purified and directly sequenced at Kunming Tsingke Biological Technology Limited Company, Kunming, Yunnan Province. All newly generated sequences were deposited at GenBank (Table 1).

Sequencher 4.6 (GeneCodes, Ann Arbor, MI, USA) was used to edit the DNA sequences. Sequences were aligned in MAFFT 7 (http://mafft.cbrc.jp/alignment/server/) using the "G–INS–i" strategy and adjusted manually in BioEdit (Hall, 1999). The sequence alignment was deposited in TreeBase (submission ID 25516). Sequences of *Gyroporus castaneus* (Bull.) Quél. and *Geastrum pseudostriatum* Hollós obtained from GenBank were used as outgroup to root trees following Crous et al. (2016) in the ITS and ITS + nLSU analyses (Figs. 1 and 2).

Maximum parsimony analyses were applied to the ITS and ITS + nLSU dataset sequences. Procedure of this analyses followed Zhao and Wu (2017), and the tree construction procedure was performed in PAUP* version 4.0b10 (Swofford, 2002). All characters were equally weighted and gaps were treated as missing data. Trees were inferred using the heuristic search option with TBR branch swapping and 1000 random sequence additions. Max-trees were set to 5000, branches of zero length were collapsed and all parsimonious trees were saved. Clade robustness was assessed using a bootstrap (BP) analysis with 1000 replicates (Felsenstein, 1985). Descriptive tree statistics tree length (TL), consistency index (CI), retention index (RI), rescaled consistency index (RC), and homoplasy index (HI) were calculated for each Maximum Parsimonious Tree (MPT) generated. Datamatrix was were also analyzed using Maximum Likelihood (ML) approach with RAxML-HPC2 software through the Cipres Science Gateway (www.phylo.org; Miller et al., 2009). Branch support (BS) for ML analysis was determined through 1000 bootstrap replicates.

MrModeltest 2.3 (Nylander, 2004) was used to determine the best-fit evolution model for the each data set for Bayesian inference (BI). Bayesian inference was calculated with MrBayes 3.1.2

Table 1
List of species, specimens, and GenBank accession numbers of sequences used in this study.

Species name	Sample no.	GenBank accession no.		References
		ITS	nLSU	
Geastrum pseudostriatum	MJ 7573	KC581992	KC581992	Jeppson, Nilsson, and Larsson (2013)
G. pseudostriatum	BP 22110	NR132884	–	Jeppson et al. (2013)
Gyroporus castaneus	JMP 0028	EU819468	EU819468	Palmer, Lindner, and Volk (2008)
Tubulicrinis angustus	109638	UDB 031055	–	Direct submision
T. angustus	NOCOR463-18	UDB 038268	–	Direct submision
T. australis	MA 88838	KX017591	KX017591	Crous et al. (2016)
T. chaetophorus	UC 2023055	KP814255	KP814255	Crous et al. (2016)
T. chaetophorus	UC 2023059	KP814233	KP814233	Crous et al. (2016)
T. glebulosus	UC 2023160	KP814394	KP814394	Crous et al. (2016)
T. glebulosus	UC 2023117	KP814297	KP814297	Crous et al. (2016)
T. glebulosus	UC 2022883	KP814234	KP814234	Crous et al. (2016)
T. globisporus	3156b	DQ873655	DQ873655	Larsson et al. (2006)
T. gracillimus	PDD 95851	HQ533047	HQ533047	Crous et al. (2016)
T. hirtellus	2040b	DQ873657	DQ873657	Larsson et al. (2006)
T. inornatus	1601b	DQ873659	DQ873659	Larsson et al. (2006)
T. martinicensis	LIP 12206	NR163282	–	Gruhn et al. (2016)
T. medius	109678	UDB031112	–	Direct submision
T. medius	NOCOR200-18	UDB038171	–	Direct submision
T. subulatus	UC 2022996	KP814455	KP814455	Crous et al. (2016)
T. subulatus	UC 2023142	KP814287	KP814287	Crous et al. (2016)
T. subulatus	UC 2022982	KP814235	KP814235	Crous et al. (2016)
T. subulatus	UC 2022890	KP814199	KP814199	Crous et al. (2016)
T. xantha	CLZhao 2868	MT153874	MT153881	Present study
T. xantha	CLZhao 2869	MT153875	MT153882	Present study
T. xantha	CLZhao 2883	MT153876	MT153883	Present study
T. yunnanensis	CLZhao 2633	MT153877	MT153884	Present study
T. yunnanensis	CLZhao 2676	MT153878	MT153885	Present study
T. yunnanensis	CLZhao 3418	MT153879	MT153886	Present study
T. yunnanensis	CLZhao 9717	MT153880	MT153887	Present study

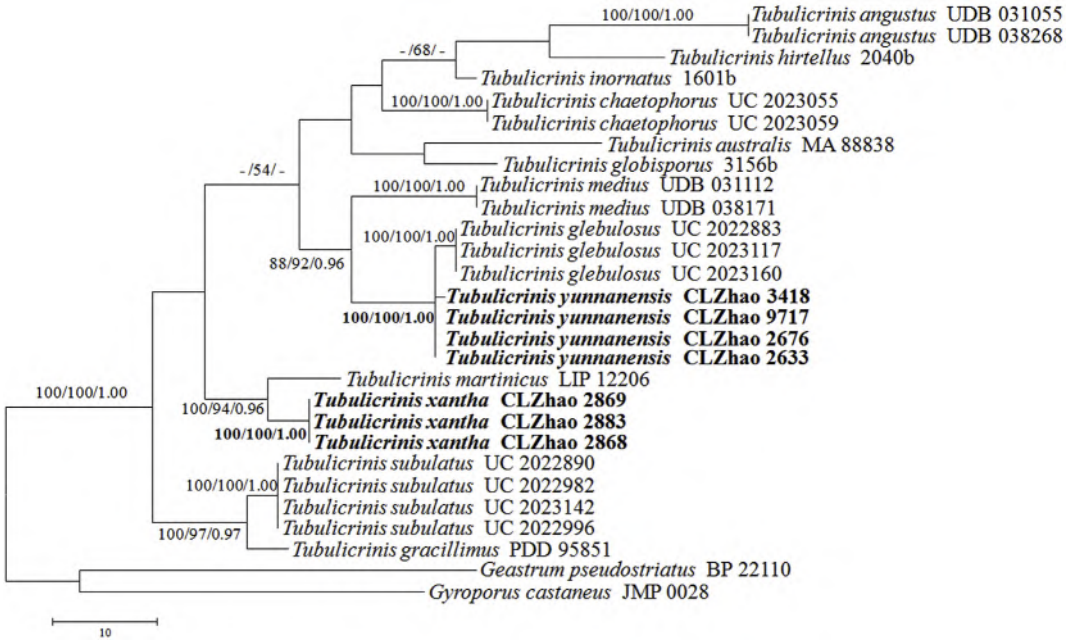

Fig. 1. Maximum parsimony strict consensus tree illustrating the phylogeny of two new species and related species in *Tubulicrinis* based on ITS sequences. Branches are labelled with maximum likelihood bootstrap >70%, parsimony bootstrap >50% and Bayesian posterior probabilities >0.95, respectively.

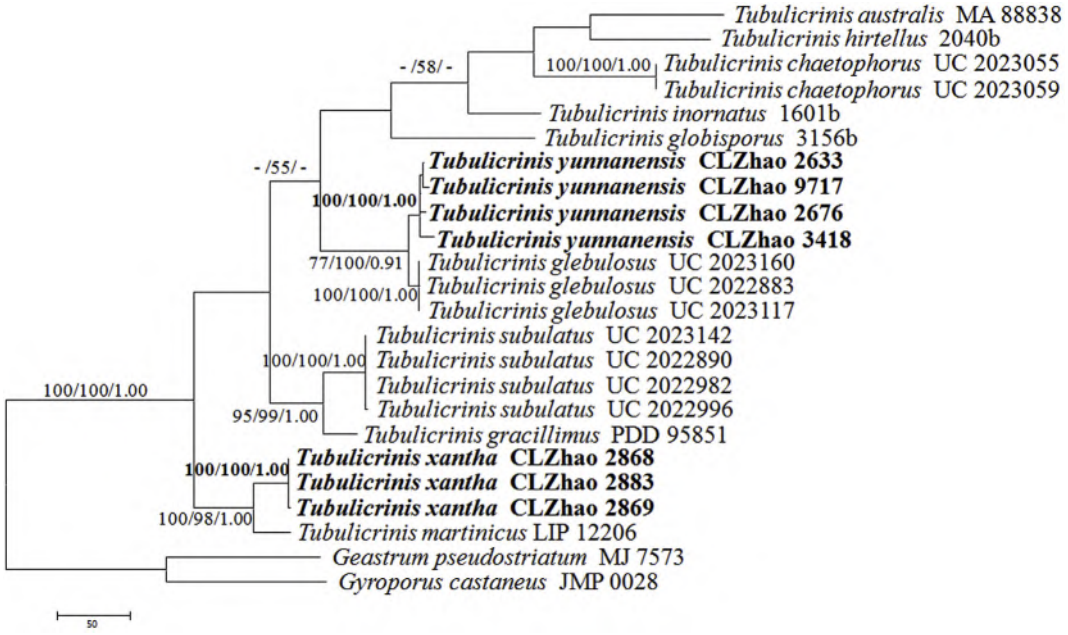

Fig. 2. Maximum parsimony strict consensus tree illustrating the phylogeny of two new species and related species in *Tubulicrinis* based on ITS + nLSU sequences. Branches are labelled with maximum likelihood bootstrap >70%, parsimony bootstrap >50% and Bayesian posterior probabilities >0.95, respectively.

(Ronquist & Huelsenbeck, 2003). Four Markov chains were run for 2 runs from random starting trees for 1 million generations on ITS dataset (Fig. 1), for 1 million generations on ITS + LSU dataset (Fig. 2), and trees were sampled every 100 generations. Beginning one-fourth of generations were discarded as burn-in. A majority rule consensus tree of all remaining trees was calculated. Branches were considered as supported if they received maximum likelihood bootstrap (BS) > 70%, maximum parsimony bootstrap (MP) > 50%, or Bayesian posterior probability (BPP) > 0.95.

3. Results

3.1. Taxonomy

Tubulicrinis xantha C.L. Zhao, sp. nov. Figs. 3 and 5.

MycoBank no.: MB 834731.

Holotype: China, Yunnan Province, Kunming, Xishan District, Haikou Forestry Park, on fallen branch of *Pinus yunnanensis* Franch., 15 Sep 2017, CLZhao 2868 (SWFC).

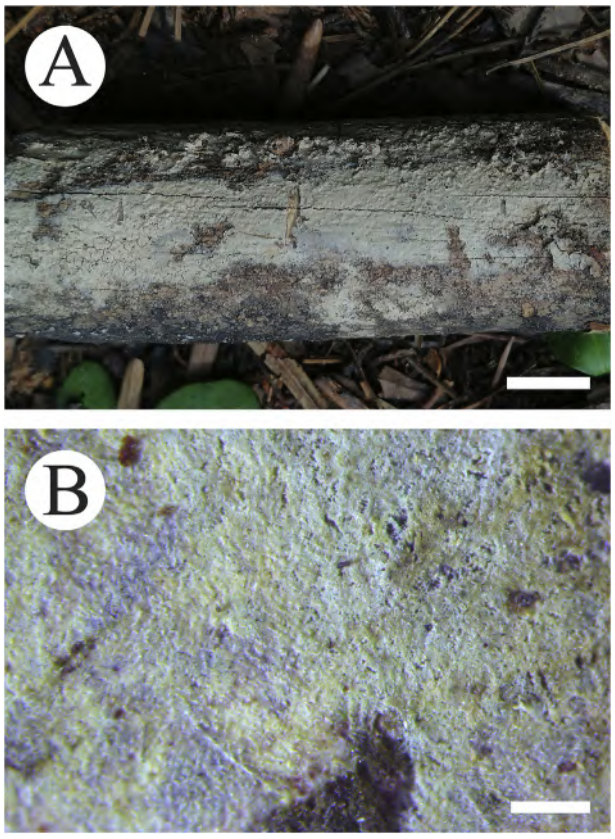

Fig. 3. Basidiomata of *Tubulicrinis xantha* (holotype). *Bars*: A 1 cm; B 0.5 mm.

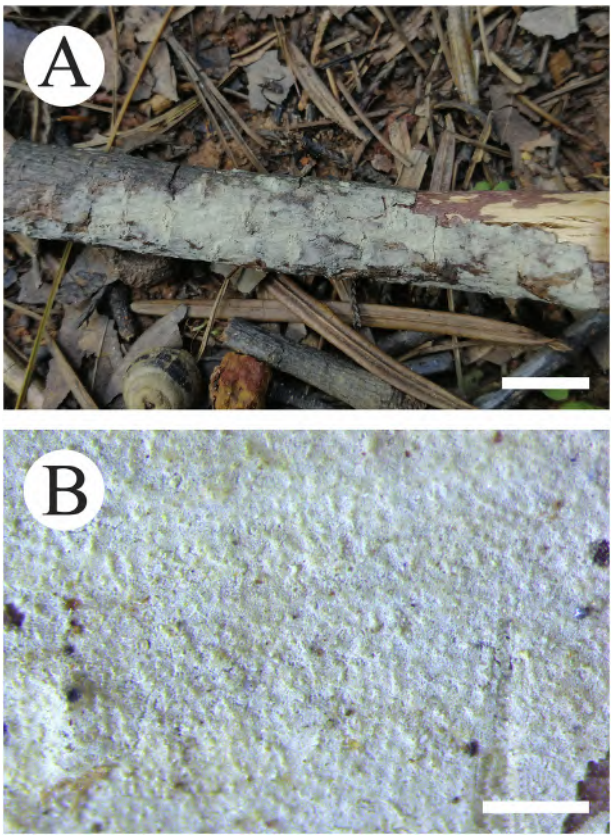

Fig. 4. Basidiomata of *Tubulicrinis yunnanensis* (holotype). *Bars*: A 1 cm; B 0.5 mm.

Etymology: *xantha* (Lat.): referring to the buff to yellowish hymenial surface.

Basidiomata: Annual, resupinate, thin, adnate, furfuraceous, without odor or taste when fresh, becoming pruinose upon drying, to 15 × 5 cm long, 50–200 μm thick. Hymenial surface smooth, yellow when fresh, turn to yellow to buff upon drying, cracked. Sterile margin unconspicuous, concolorous with hymenial surface.

Hyphal structure: Monomitic; generative hyphae with clamp connections, hyaline, thin-walled, branched, 1.5–3 μm in diam.; IKI–, CB–, tissues unchanged in KOH.

Hymenium: Lyocystidia numerous, projecting, cylindrical to slightly sinuous, bi-rooted, dissoving in KOH, amyloid, capillary lumen ending gradually, 78–192.5 × 5.8–7.5 μm and cystidioles absent; basidia small, clavate, thin-walled, with four sterigmata and a basal clamp connection, 8–14.5 × 2.5–3.5 μm; basidioles dominant, in shape similar to basidia, but slightly smaller.

Basidiospores: Cylindrical to allantoid, hyaline, thin-walled, smooth, IKI–, CB–, (5–)5.3–6.3(–6.5) × 1.2–1.6 μm, L = 5.94 μm, W = 1.45 μm, Q = 3.94–4.12 (n = 90/3).

Additional specimens examined: CHINA, Yunnan Province, Kunming, Xishan District, Haikou Forestry Park, on fallen branch of *Pinus yunnanensis*, 15 Sep 2017, CLZhao 2869, CLZhao 2883 (SWFC).

Tubulicrinis yunnanensis C.L. Zhao, sp. nov. Figs. 4 and 6.

MycoBank no.: MB 834732.

Holotype: China, Yunnan Province, Puer, Jingdong County, Wuliangshan National Reserve Nature, on fallen branch of angiosperm, 6 Jul 2019, CLZhao 9717 (SWFC).

Etymology: *yunnanensis* (Lat.): referring to the locality (Yunnan Province) of the type specimens.

Basidiomata: Annual, resupinate, thin, adnate, without odor or taste when fresh, becoming pruinose up on drying, to 10 × 4 cm long, 100–250 μm thick. Hymenial surface smooth, cream to primrose when fresh, turn to primrose to olivaceous buff upon drying. Sterile margin unconspicuous, concolorous with hymenial surface.

Hyphal system: Monomitic; generative hyphae with clamp connections, hyaline, thin-walled, branched, 1.5–3.5 μm in diam.; IKI–, CB–, tissues unchanged in KOH.

Hymenium: Lyocystidia numerous, cylindrical, bi-rooted, dissoving in KOH, amyloid, capillary lumen ending gradually, encrusted, 46–160 × 6.2–10 μm and cystidioles absent; basidia small, clavate, thin-walled, with four sterigmata and a basal clamp connection, 8.5–20.5 × 2.5–4.5 μm; basidioles dominant, in shape similar to basidia, but slightly smaller.

Basidiospores: Cylindrical, hyaline, thin-walled, smooth, multiguttulate, IKI–, CB–, (8–)4.2–6.2(–6.5) × 1.2–2 μm, L = 5.55 μm, W = 1.62 μm, Q = 2.9–3.59 (n = 120/4).

Additional specimens examined: CHINA, Yunnan Province, Yuxi, Xinping County, Mopanshan National Forestry Park, on the trunk of *Albizia julibrissin* Durazz, 20 Aug 2017, CLZhao 2633; on the angiosperm trunk, 20 Aug 2017, CLZhao 2676; Puer, Zhenyuan Country, Xieqipo Park, on the fallen branch of angiosperm, 1 Oct 2017, CLZhao 3418 (SWFC).

3.2. Molecular phylogeny

The ITS dataset included sequences from 28 fungal specimens representing 15 taxa. It had an aligned length of 755 characters in the dataset, of which 266 characters are constant, 149 are variable parsimony-uninformative, and 340 are parsimony-informative. Maximum parsimony analysis yielded 6 equally parsimonious trees (TL = 305, CI = 0.550, HI = 0.449, RI = 0.667, RC = 0.367). Best

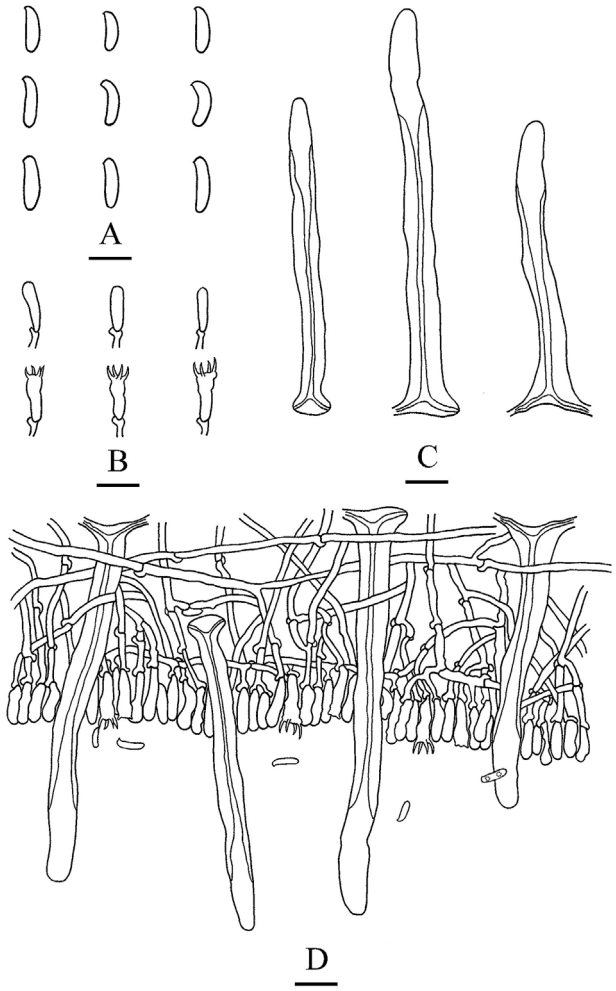

Fig. 5. Microscopic structures of *Tubulicrinis xantha* (draw from the holotype). A: Basidiospores. B: Basidia and basidioles. C: Cystidia. D: A section of hymenium. *Bars*: A 5 μm; B–D 10 μm.

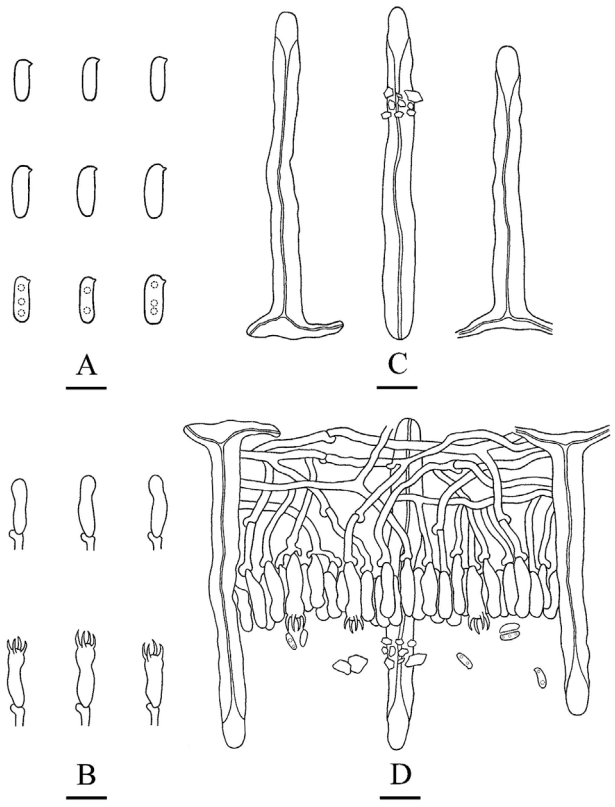

Fig. 6. Microscopic structures of *Tubulicrinis yunnanensis* (draw from the holotype). A: Basidiospores. B: Basidia and basidioles. C: Cystidia. D: A section of hymenium. *Bars*: A 5 μm; B–D 10 μm.

model for ITS estimated and applied in the Bayesian analysis: GTR + I + G, lset nst = 6, rates = invgamma; prset statefreqpr = dirichlet (1,1,1,1). Bayesian analysis resulted in the similar topology to MP analysis with an average standard deviation of split frequencies = 0.004255, and the effective sample size (ESS) across the two runs is the double of the average ESS (avg ESS) = 364.5.

The phylogeny (Fig. 1) inferred from ITS sequences demonstrated that *Tubulicrinis xantha* grouped with *T. martinicensis* G. Gruhn, G. Gruhn, Hallenb. & Courtec., and *T. yunnanensis* was sister with *T. glebulosus* (Fr.) Donk.

The ITS + nLSU dataset (Fig. 2) included sequences from 24 fungal specimens representing 13 species. The dataset had an aligned length of 2165 characters, of which 1470 characters are constant, 306 are variable and parsimony-uninformative, and 389 are parsimony-informative. Maximum parsimony analysis yielded 84 equally parsimonious trees (TL = 1502, CI = 0.6798, HI = 0.3202, RI = 0.6971, RC = 0.4739). Best model for the ITS + nLSU dataset estimated and applied in the Bayesian analysis: GTR + I + G, lset nst = 6, rates = invgamma; prset statefreqpr = dirichlet (1,1,1,1). Bayesian analysis and ML analysis resulted in a similar topology as MP analysis, with an average standard deviation of split frequencies = 0.006311 (BI) and the effective sample size (ESS) across the two runs is the double of the average ESS (avg ESS) = 698.5.

Also here (Fig. 2), *T. xantha* grouped with *T. martinicensis*, and *T. yunnanensis* with *T. glebulosus* in strongly supported clades.

In addition, the results of BLAST queries in NCBI for *T. yunnanensis* based on ITS separately showed the sequences producing significant alignments descriptions: the top five taxa are *T. glebulosus* (Maximum record descriptions: Max score 992; Total score 992; Query cover 95%; E value 0; Ident 96.39%); for *T. xantha* based on ITS separately showed the sequences producing significant alignments descriptions: the top five taxa is *T. martinicensis* (Maximum record descriptions: Max score 721; Total score 721; Query cover 89%; E value 0; Ident 91.13%).

4. Discussion

In the present study, two new species, *T. xantha* and *T. yunnanensis* are described based on phylogenetic analyses and morphological characters.

Phylogenetically, *T. xantha* grouped with *T. martinicensis*, and *T. yunnanensis* was sister with *T. glebulosus* (Figs. 1 and 2). However, morphologically, *T. martinicensis* differs from *T. xantha* by its basidiomata cracking into pieces and light ochraceous hymenial surface (Gruhn et al., 2016). *Tubulicrinis glebulosus* differs from *T. yunnanensis* by the flocculose to granular hymenophore, white to ochraceous hymenial surface and larger basidiospores (6–9 × 1.5–2.25 μm, Donk, 1956).

Tubulicrinis xantha is similar to two species of *Tubulicrinis* based on having cylindrical to slightly sinuous lyocystidia (*T. angustus* (D.P. Rogers & Weresub) Donk, Telleria & M.P. Martín and *T. medius* (Bourdot & Galzin) Oberw.). However, morphologically *T. angustus* differs from *T. xantha* by the white hymenial surface and larger basidiospores (8–11 × 1.8–2.5 μm, Donk, 1956); *T. medius* by the

porulose to granulose basidiomata with white hymenial surface (Oberwinkler, 1966).

Tubulicrinis yunnanensis shares the encrusted cystidia with five related species in *Tubulicrinis* (*T. australis* M. Dueñas, *T. borealis* J. Erikss., *T. calothrix* (Pat.) Donk, *T. hirtellus* (Bourdot & Galzin) J. Erikss and *T. subulatus* (Bourdot & Galzin) Donk), but morphologically *T. australis* differs from *T. yunnanensis* by the poroid to reticulate basidiomata with white to cream hymenial surface and wider basidiospores (6–7.5 × 3–3.5 μm, Crous et al., 2016). *Tubulicrinis borealis* differs in its whitish to ochraceous hymenial surface, thick-walled generative hyphae and strongly amyloid basidia (Eriksson, 1958). *Tubulicrinis calothrix* differs in its rimose hymenophore and larger basidiospores (6–8 × 1.5–2 μm, Donk, 1956). *Tubulicrinis hirtellus* is separated from *T. yunnanensis* by its larger basidiospores (7–8.5 × 2–2.5 μm, Eriksson, 1958). *Tubulicrinis subulatus* by the pilose basidiomata with whitish to cream or yellowish brown hymenial surface and subulate cystidia (Donk, 1956).

In geographical distribution, *Tubulicrinis* species are an extensively studied group of Basidiomycota (Bernicchia & Gorjón, 2010; Crous et al., 2016; Dai, 2011), and six species of *Tubulicrinis* were recorded in China (Dai, 2011). However, the wood-rotting fungi diversity is still not well known, especially in East Asia areas. Many recently described taxa of wood-rotting fungi were from these areas (Bian & Dai, 2015; Chen, Korhonen, Li, & Dai, 2014; Cui et al., 2019; Dai, 2012; Han & Cui, 2015; Li & Cui, 2013; Shen et al., 2019; Song, Chen, Wang, Chen, & Cui, 2016; Zhu, Song, Zhou, Si, & Cui, 2019). Two new species in the present study, *T. xantha* and *T. yunnanensis*, are from East Asia, too.

Declaration of competing interestCOI

The authors declare no conflict of interest. All the experiments undertaken in this study comply with the current laws of the People's Republic of China.

Acknowledgements

The research was supported by the National Natural Science Foundation of China (Project No. 31700023), and Yunnan Agricultural Foundation Projects (2017FG001-042), and the Key Laboratory of State Forestry Adminstration for Highly-Efficient Utilization of Forestry Biomass Resources in Southwest China (Southwest Forestry University) (Project No. 2019-KF10).

References

Bernicchia, A., & Gorjón, S. P. (2010). *Fungi Europaei 12: Corticiaceae s.l.* Alassio: Edizioni Candusso.

Bian, L. S., & Dai, Y. C. (2015). *Coltriciella globosa* and *C. pseudodependens* spp. nov. (Hymenochaetales) from southern China based on morphological and molecular characters. *Mycoscience, 56*, 190–197. https://doi.org/10.1016/j.myc.2014.06.001.

Chen, J. J., Korhonen, K., Li, W., & Dai, Y. C. (2014). Two new species of the *Heterobasidion insulare* complex based on morphology and molecular data. *Mycoscience, 55*, 289–298. https://doi.org/10.1016/j.myc.2013.11.002.

Crous, P. W., Wingfield, M. J., Burgess, T. I., Hardy, G. E. S. J., Crane, C., Barrett, S., et al. (2016). Fungal planet description sheets: 469–557. *Persoonia, 37*, 218–403. https://doi.org/10.3767/003158516X694499.

Cui, B. K., Li, H. J., Ji, X., Zhou, J. L., Song, J., Si, J., et al. (2019). Species diversity, taxonomy and phylogeny of Polyporaceae (Basidiomycota) in China. *Fungal Diversity, 97*, 137–392. https://doi.org/10.1007/s13225-019-00427-4.

Cunningham, G. H. (1963). The Thelephoraceae of Australia and New Zealand. *Bulletin of the New Zealand Department of Industrial Research, 145*, 1–359.

Dai, Y. C. (2011). A revised checklist of corticioid and hydnoid fungi in China for 2010. *Mycoscience, 52*, 69–79. https://doi.org/10.1007/S10267-010-0068-1.

Dai, Y. C. (2012). Polypore diversity in China with an annotated checklist of Chinese polypores. *Mycoscience, 53*, 49–80. https://doi.org/10.1007/s10267-011-0134-3.

Donk, M. A. (1956). Notes on resupinate Hymenomycetes: III. *Fungus, 26*, 3–24.

Eriksson, J. (1958). Studies in the Heterobasidiomycetes and Homobasidiomycetes-Aphyllophorales of Muddus National Park in North Sweden. *Symbolae Botanicae Upsalienses, 16*, 1–172.

Felsenstein, J. (1985). Confidence intervals on phylogenetics: An approach using bootstrap. *Evolution, 39*, 783–791. https://doi.org/10.1111/j.1558-5646.1985.tb00420.x.

Gruhn, G., Hallenberg, N., & Courtecuisse, R. (2016). *Tubulicrinis martinicensis* sp. nov., a corticioid species from Martinique (French West Indies). *Mycotaxon, 131*, 631–638. https://doi.org/10.5248/131.631.

Hall, T. A. (1999). BioEdit: A user-friendly biological sequence alignment editor and analysis program for Windows 95/98/NT. *Nucleic Acids Symposium Series, 41*, 95–98.

Han, M. L., & Cui, B. K. (2015). Morphological characters and molecular data reveal a new species of *Fomitopsis* (Polyporales) from southern China. *Mycoscience, 56*, 168–176. https://doi.org/10.1016/j.myc.2014.05.004.

Hayashi, Y. (1974). Studies on the genus *Peniophora* Cke. and its allied genera in Japan. *Bulletin of the Government Forest Experimental Station Meguro, 260*, 1–98.

Hjortstam, K. (1981). Notes on Corticiaceae (Basidiomycetes) VIII. Two new species of Tubulicrinis. *Mycotaxon, 13*, 120–123.

Hjortstam, K. (2001). Tubulicrinaceae, a survey of the genera and species. *Windahlia, 24*, 1–14.

Hjortstam, K., Larsson, K. H., Ryvarden, L., & Eriksson, J. (1988). *The corticiaceae of North Europe* (Vol. 8). Oslo: Fungiflora.

Jeppson, M., Nilsson, R. H., & Larsson, E. (2013). European earthstars in Geastraceae (Geastrales, Phallomycetidae) – a systematic approach using morphology and molecular sequence data. *Systematics and Biodiversity, 11*, 437–465. https://doi.org/10.1080/14772000.2013.857367.

Larsson, K. H., Parmasto, E., Fischer, M., Langer, E., Nakasone, K. K., & Redhead, S. A. (2006). Hymenochaetales: A molecular phylogeny for the hymenochaetoid clade. *Mycologia, 98*, 926–936. https://doi.org/10.1080/15572536.2006.11832622.

Li, H. J., & Cui, B. K. (2013). Two new *Daedalea* species (Polyporales, Basidiomycota) from South China. *Mycoscience, 54*, 62–68. https://doi.org/10.1016/j.myc.2012.07.005.

Miller, M. A., Holder, M. T., Vos, R., Midford, P. E., Liebowitz, T., Chan, L., et al. (2009). The CIPRES portals. *CIPRES*. URL http://www.phylo.org/sub_sections/portal http://www.webcitation.org/5imQlJeQa (Archived by WebCite(r) at.

Nylander, J. A. A. (2004). *MrModeltest v2. Program distributed by the author*. Uppsala: Evolutionary Biology Centre, Uppsala University.

Oberwinkler, F. (1966). Die battung *Tubulicrinis* Donk s.l. *Zeitschrift für Pilzkunde, 31*, 12–48. https://doi.org/10.1007/BF02312715.

Palmer, J. M., Lindner, D. L., & Volk, T. J. (2008). Ectomycorrhizal characterization of an American chestnut (*Castanea dentata*)-dominated community in Western Wisconsin. *Mycorrhiza, 19*, 27–36. https://doi.org/10.1007/s00572-008-0200-7.

Petersen, J. H. (1996). Farvekort. The Danish mycological society's colour-chart. *Greve: Foreningen til Svampekundskabens Fremme*.

Rajchenberg, M. (2002). Corticioid and polyporoid fungi (Basidiomycota) that decay *Austrocedrus chilensis* in Patagonia, Argentina. *Mycotaxon, 81*, 215–227.

Ronquist, F., & Huelsenbeck, J. P. (2003). Mrbayes 3: Bayesian phylogenetic inference under mixed models. *Bioinformatics, 19*, 1572–1574. https://doi.org/10.1093/bioinformatics/btg180.

Ryvarden, L. (1975). Studies in the Aphyllophorales of africa 2. Some new species from East africa. *Norwegian Journal of Botany, 22*, 25–34.

Sharma, J., Singh, A. P., & Dhingra, G. S. (2015). *Tubulicrinis indicus*, a new corticioid species from India. *Mycotaxon, 130*, 879–881. https://doi.org/10.5248/130.879.

Shen, L. L., Wang, M., Zhou, J. L., Xing, J. H., Cui, B. K., & Dai, Y. C. (2019). Taxonomy and phylogeny of *Postia*. Multi-gene phylogeny and taxonomy of the brown-rot fungi: *Postia* and its related genera. *Persoonia, 42*, 101–126. https://doi.org/10.3767/persoonia.2019.42.05.

Song, J., Chen, J. J., Wang, M., Chen, Y. Y., & Cui, B. K. (2016). Phylogeny and biogeography of the remarkable genus *Bondarzewia* (Basidiomycota, Russulales). *Scientific Reports, 6*, 34568. https://doi.org/10.1038/srep34568.

Swofford, D. L. (2002). *PAUP*: Phylogenetic analysis using parsimony (*and other methods). Version 4.0b10*. Sunderland, Massachusetts: Sinauer Associates.

White, T. J., Bruns, T., Lee, S., & Taylor, J. (1990). Amplification and direct sequencing of fungal ribosomal RNA genes for phylogenetics. In M. A. Innis, D. H. Gelfand, J. J. Sninsky, & T. J. White (Eds.), *PCR protocols: A guide to methods and applications (pp 315–322)*. San Diego: Academic Press. https://doi.org/10.1016/B978-0-12-372180-8.50042-1.

Zhao, C. L., & Wu, Z. Q. (2017). *Ceriporiopsis kunmingensis* sp. nov. (Polyporales, Basidiomycota) evidenced by morphological characters and phylogenetic analysis. *Mycological Progress, 16*, 93–100. https://doi.org/10.1007/s11557-016-1259-8.

Zhu, L., Song, J., Zhou, J. L., Si, J., & Cui, B. K. (2019). Species diversity, phylogeny, divergence time and biogeography of the genus *Sanghuangporus* (Basidiomycota). *Frontiers in Microbiology, 10*, 812. https://doi.org/10.3389/fmicb.2019.00812.